



LAWRENCE  
LIVERMORE  
NATIONAL  
LABORATORY

# Microscale Metrology and Assembly Using Standing Wave Probes

M. Bauza, R. Seugling, S. Woody, B. Nowakowski, S.  
Smith, I. Darnell, J. Florando, P. Fitsos

July 22, 2008

The 3rd International Conference on MicroManufacturing  
Pittsburgh, PA, United States  
September 9, 2008 through September 11, 2008

## **Disclaimer**

---

This document was prepared as an account of work sponsored by an agency of the United States government. Neither the United States government nor Lawrence Livermore National Security, LLC, nor any of their employees makes any warranty, expressed or implied, or assumes any legal liability or responsibility for the accuracy, completeness, or usefulness of any information, apparatus, product, or process disclosed, or represents that its use would not infringe privately owned rights. Reference herein to any specific commercial product, process, or service by trade name, trademark, manufacturer, or otherwise does not necessarily constitute or imply its endorsement, recommendation, or favoring by the United States government or Lawrence Livermore National Security, LLC. The views and opinions of authors expressed herein do not necessarily state or reflect those of the United States government or Lawrence Livermore National Security, LLC, and shall not be used for advertising or product endorsement purposes.

# Microscale Metrology and Assembly Using Standing Wave Probes

ICOMM  
2008  
No.: 75

Marcin B. Bauza<sup>1\*</sup>, Richard M. Seugling<sup>3</sup>, Shane C. Woody<sup>1</sup>, Bartosz K. Nowakowski<sup>2</sup>,  
Stuart T. Smith<sup>2</sup>, Ian M Darnell<sup>3</sup>, Jeffery N. Florando<sup>3</sup>, and Peter J. Fitsos<sup>3</sup>

<sup>1</sup>InsituTec Inc., 2750 East W.T. Harris Blvd, Suite 103, Charlotte, NC, USA, 28213

<sup>2</sup>Center for Precision Metrology, UNCC ERB Bldg, 9201 University City Blvd, Charlotte, NC, USA, 28223

<sup>3</sup>Lawrence Livermore National Laboratory 7000 East Ave, Livermore, CA, USA 94551

## INTRODUCTION

Measurement and assembly of microscale components continues to remain a challenging problem using current state of the art micro-tools. For example to measure small features such as holes, pins or channels; AFM, SPM, or SEM [1][2][3] are frequently used. However, these tools are more applicable for surface finish measurement and lack the ability to make dimensional measurements on high aspect ratio features. As a result, various new microscale probing systems have been developed over the past few years for the metrology industry. Nonetheless, challenging problems remain such as adhesion interaction between the probe tip and measured surface [4][5], inherent scaling issues and lack of ability to perform uninterrupted scanning. In microscale robotics, pick and place tools also experience inherent scaling affects such as inability to pick and release parts due to attraction forces. In both the case of metrology and pick and place, adhesion interactions greatly influence the performance of the tool. The objective of this proposed paper is to discuss a new class of nano and microscale tool referred to as standing wave probes. This technology was originally discussed as a metrology tool at the 2005 and 2006 ASPE annual conference. Continued work over the past 18 months has progressed in modeling surface-tip interactions, scaling affects to nanoscale, tip energetics (i.e. energy at the tip) as well as reduction to practice in microscale metrology and robotic pick and place tools. Three categories proposed in this paper are briefly discussed further in modeling, metrology and pick and place.

## MODELING

To address the potential application of this technology for use on micrometer-scale, high aspect ratio features as well as a pick and place tool, a detailed understanding of the probe dynamics coupled with the nonlinear contact interactions is required. A set of complex numerical models have been derived to incorporate the drive/sensor piezoelectric effect, dynamics of the probe fiber and surface interactions between the probe tip and surface. Modeling of the complete system has been a combination of finite element analysis and numerical integration to account for the complex nonlinear surface contact effects. This system has been broken down into four

subsystems including the piezoelectric tuning fork driver/sensor, electronic sensing/drive circuits, beam dynamics and surface force interactions. Nonlinearities of the system are primarily dictated by the surface interaction of the probe tip as it comes into contact with the workpiece. Integrated within the model boundary conditions at the probe are elastic and inelastic impact [6], meniscus, air damping, electrostatic, and Van der Waals and adhesion forces [7][8].

Because of the complexity of the dynamic interaction between the oscillating fiber (probe) and the surface, the system was modeled numerically in FORTRAN using Euler–Bernoulli beams for the fiber, piezoelectric beams for the tuning fork tines [9]. Included in the numerical model are the drive electronics and the nonlinear boundary conditions. A schematic illustration of the model is shown in Fig. 1. In addition, COMSOL multiphysics finite element analysis (FEA) package was used to verify modes and sensitivity of the tuning fork.

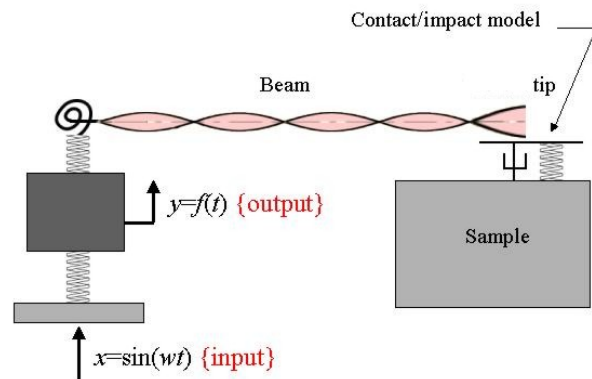


**Figure 1.** Schematic illustration of the numerical model derived representing the probe system dynamics and contact with a surface.

To verify that the model represents our system, the first task was to compare the frequency response of the model in the free-state (i.e. noncontact) with the experimental data, results of which are shown in Fig. 2. In this case, material properties, geometry and electronics parameters are quantitatively meas-

\* Corresponding Author: marcin.bauza@insitutec.com

ured and included in the calculation. However, damping of both the material and viscous effects of operating in air are “tuned” to properly represent probe dynamics in an air environment.

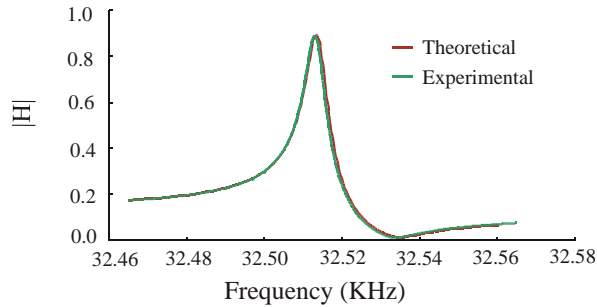


**Figure 2.** Theoretical and experimental frequency response of the probe system.

To validate the sensitivity of the tuning fork to applied voltage a nanoindenter was used to simultaneously measure load and displacement, see Fig. 3. The results were compared to the COMSOL FEA model with an agreement of better than 10% and a strain sensitivity of  $0.3 \text{ nm} \cdot \text{V}^{-1}$ .

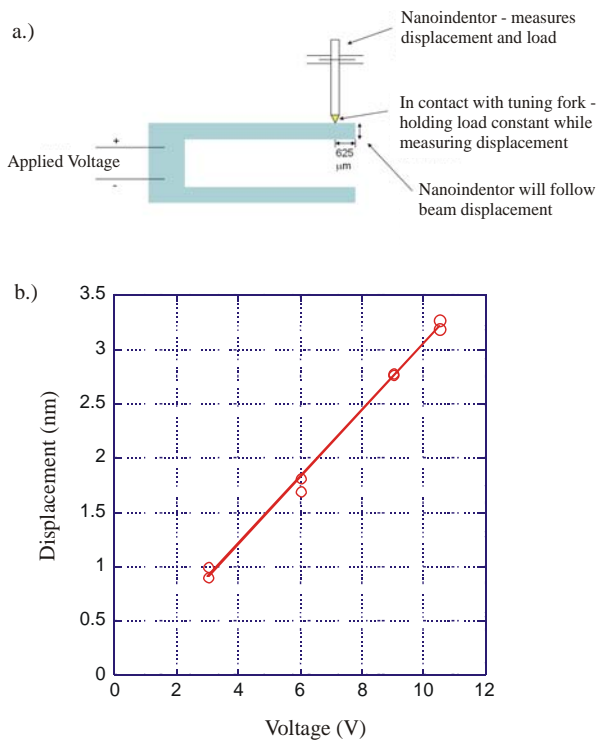


**Figure 3.** a.) Schematic representation of the nanoindenter test set-up. b.) Displacement as a function of applied voltage.

With the static and dynamic data well represented by the numerical model, the nonlinear boundary conditions of the probe tip contacting a surface were added. These include surface force effects, as mentioned earlier and an elastic and/or inelastic contact model. In general, the surface forces are dominated by meniscus effects at this probe scale. Figure 4 shows the complete model output as the probe tip comes into contact with a surface. Figure 4a are snap-shots in time of the

mode shape of the beam and tuning fork as the surface is brought into contact. It is clear that energy imparted to the probe during initial contact excites lower order modes, however the amplitude only reaches  $\sim 40 \mu\text{m}$  with a  $\pm 10 \mu\text{m}$  initial oscillation amplitude. This effect can be observed experimentally and has proven to damp out due partially to air drag damping. The low mode oscillations tend to decrease in amplitude as the surface is continually stepped into contact as can be seen in the step #3 ( $0.72 \mu\text{m}$ ) mode shape. Figure 4b is the RMS signal amplitude variation as the probe is stepped into contact with a surface as predicted by the model.

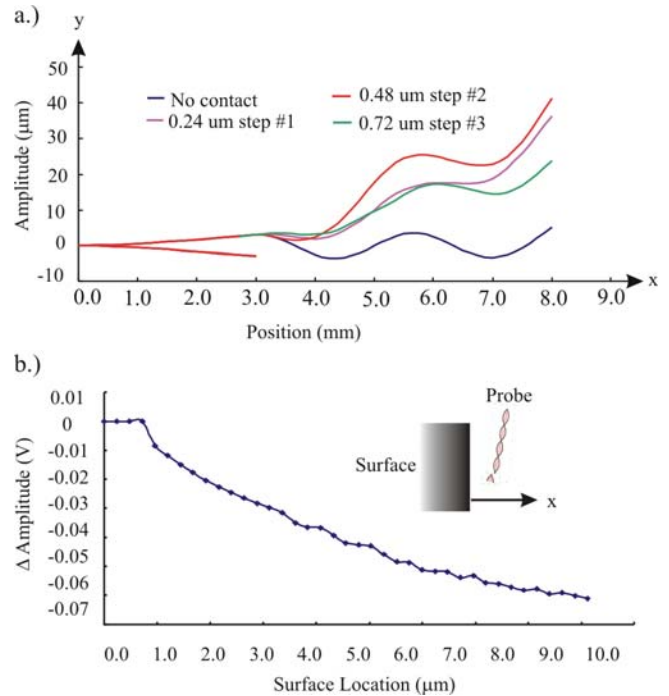


**Figure 4.** a.) Mode shape of probe as the surface is brought into contact with the probe tip. b.) Model predicted amplitude variation as the surface is brought into contact with the surface.

In general, the combination of the numerical model and the COMSOL FEA model predict the response of the system to better than 10% for the “free” and static cases. Introducing the nonlinear boundary conditions add uncertainty to model in that quantification of the relative surface force and material contributions is a bounded estimate. Surface forces were quantified experimentally using an atomic force microscope (AFM) by attaching a probe fiber tip to an AFM cantilever and measuring the forces of materials of interest, such as steel gage block and a gold foil. It has been found both analytically and experimentally that for a nominally 5.0 mm long fiber an adhesion force of  $\sim 100 \mu\text{N}$  will stick the fiber to the surface. However, oscillating the probe at a higher order mode increases the restoring force of the prestrained fiber and decreases the surface force contribution.

## MICROSCALE METROLOGY

### A. STANDING WAVE PROBE

At the moment, the standing wave probes are designed with  $> 400:1$  aspect ratio probe shanks (length to diameter), fabricated with  $7\ \mu\text{m}$  diameter widths and attached at one end to an oscillator. The oscillator produces a pronounced standing

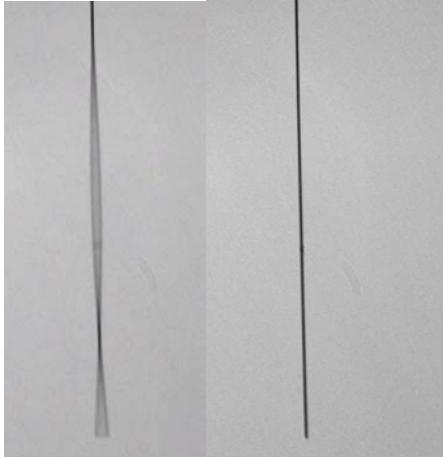


**Figure 5.** Image of the standing wave probe in “on mode” shown on the left and “off mode” show on the right

wave propagating along the probe shank and operating up to 150 kHz, Figure 5. The tip at the end is configured to swing out beyond the shaft of the fiber and is used as the single point of contact during the measurement process. Thus, the probe does not require a spherical ball (classical approach used in macroscale probing) to be attached on the end of the fiber and therefore serve as a defined point of contact during the measurement process. Moreover, as a result of the standing wave’s inertia the mechanical contact interactions between the tip and workpiece surface are not susceptible to attraction forces [1]. Measurement results using the probe in conjunction with a roundness measuring machine are discussed below. Feature sizes have demonstrated diameters less than  $130\ \mu\text{m}$  and 10 nm repeatability.

### B. ROUNDNESS MEASURING STATION

The roundness gauge unit is attached to a modified Z-axis of a Moore 1.5 machine and the 5 axis alignment system is mounted on a XY table, as well as horizontal vision system, see Figure 6. First, the Moore XY table is positioned to bring the

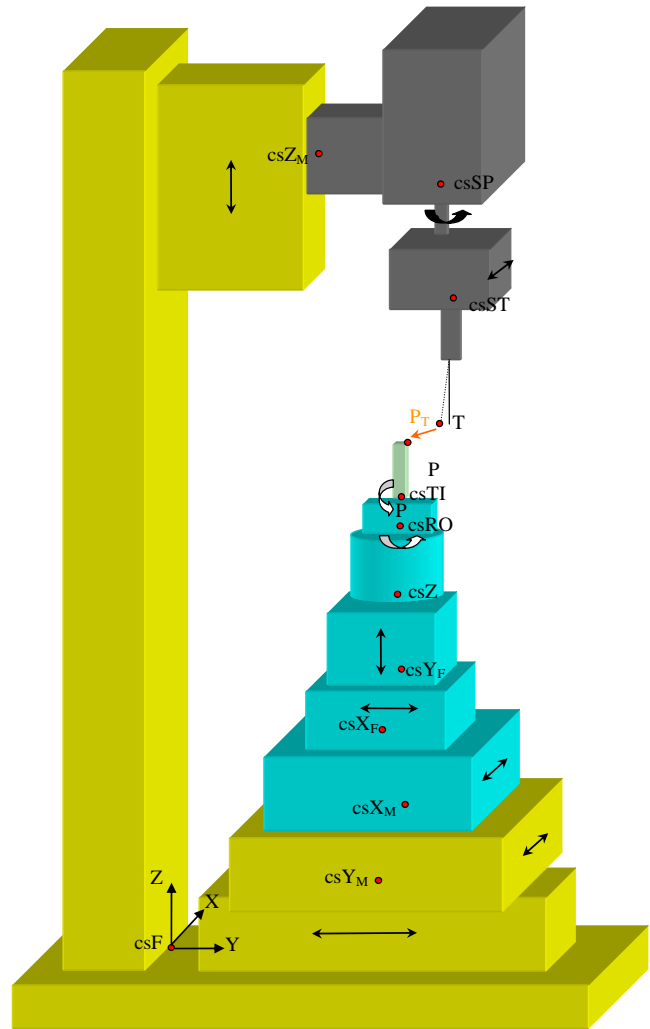


**Figure 6.** Simplified model of the roundness apparatus used during test measurements

Fibermax into the same working envelop as the roundness gauge. Next, the FiberMax is used to move and align the measured component. Once the alignment sequence is completed, the probe is contacted against the specimen and closed loop controlled at a constant applied force. The roundness gauge is then rotated about the specimen and the fiber probe is scanned normal along the surface. The encoder signal and scanning head displacement are simultaneously measured and synchronized together [11]. This enables the operator to measure the roundness of a circular feature, Figure 7. To extend this to 3D measurements, the Fibermax Z-axis is employed and simultaneously measured with the encoder and gauge head displacement.

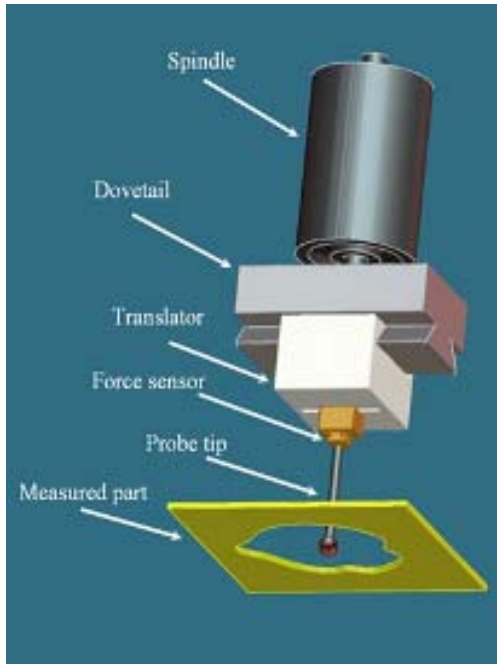


**Figure 7.** Schematic of constant force measurement technique applied to roundness measuring machine

### C. MEASUREMENTS OF MICROSCALE OD AND ID SHAPES

To demonstrate the metrological capability of the standing wave sensor many test were conducted on both flat and round surfaces. However, due to space limitations authors will present only two examples, one of 250  $\mu\text{m}$  OD 3D measurements, and second of 128  $\mu\text{m}$  ID repeatability measurements. For the OD measurements a steel dowel pin was chosen and its end was purposely sheared to show taper, Figure 8. The standing wave sensor was used to measure the shape of the pin at 4 heights equispaced by 50  $\mu\text{m}$  a part from each other. Two of these measurements were on the tapered region of the pin as observed in, Figure 9. The scan was performed with a speed of 2 RPM and each scan contains 1000 equally spaced points.

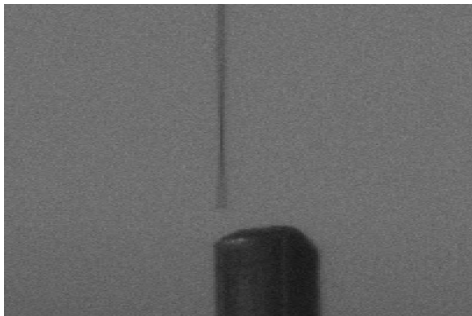


**Figure 8.** Image of standing wave probe above 250  $\mu\text{m}$  dove pin pin.

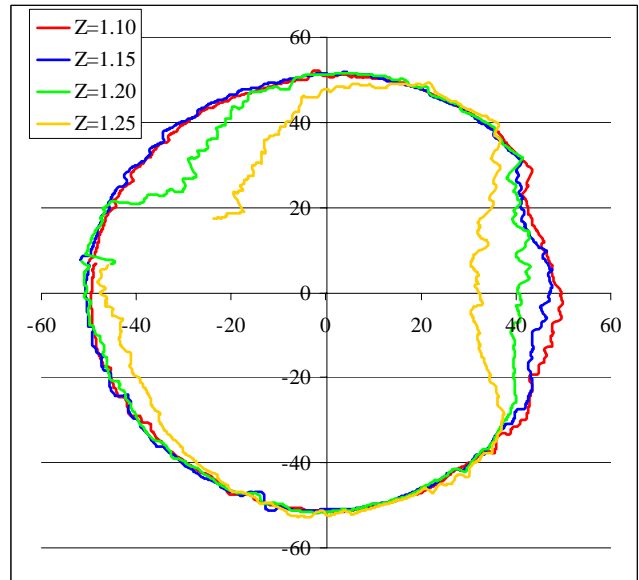


**Figure 9.** 3D image of the roundness data described on 50  $\mu\text{m}$  circle. Colors represent different heights of consecutive roundness traces of above dove pin.

For the hole measurement a glass optic ferule BC# 2763 produced by Ozoptics Inc in Canada was chosen. The ferrule has a through hole with diameter of 128  $\mu\text{m}$ . The glass ferrule's hole was scanned at constant applied force with a bandwidth of 20 Hz and approximately 14,000 data points were collected during one revolution, Figure 10. The depth is set and limited to approximately 0.5 mm due to lack of automation in the setup and alignment. The local features, Figure 11, are highly repeatable in a range of 30 nm and the observed local misalignments are

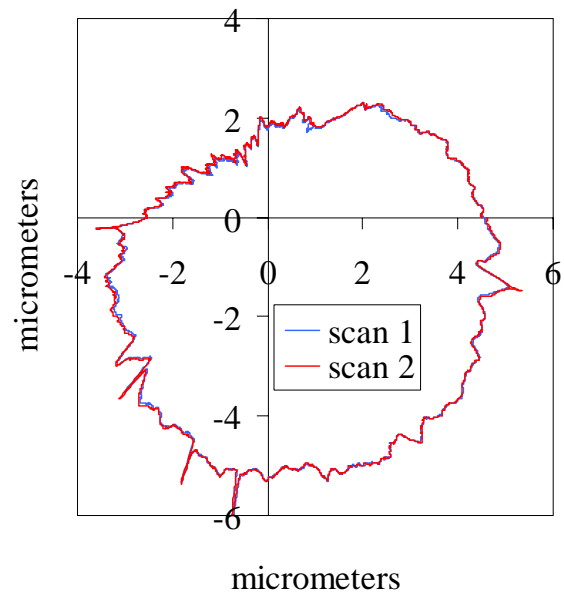


**Figure 10.** Two consecutive measurements of 128  $\mu\text{m}$  fiber optic coupler described on 4  $\mu\text{m}$  circle.

primarily related to spindle asynchronous error motion. The measurement shows a 1  $\mu\text{m}$  out of roundness of the measured

part the dominant component of which can be observed as a 2 UPR out of roundness. The repeatability of long and short wavelength features clearly demonstrates the potential of the standing wave technology in measurement of surface finish as well as dimensional values.

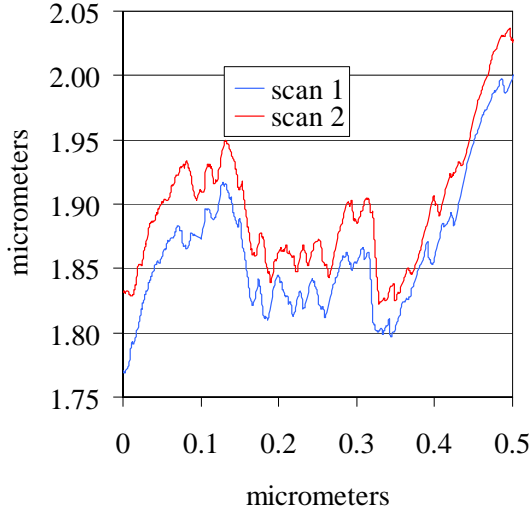


**Figure 11.** Zoom in of Fig. 6 to show surface irregularities of the fiber optic coupler.

#### MICROSCALE PICK AND PLACE

Research work was also carried out for pick and place studies. In this area, researchers employed dual standing wave probes as self sensing tweezers [12]. The objective was to evaluate using the standing wave methodology in actuated robotic ‘fingers’ to controllably pick and release specimens. In the state of the art for microscale pick and place tools, the specimens often stick to the tools due to attraction forces. To overcome the uncontrolled adhesion, standard practice is to use hierarchy of adhesive materials, such as GelPak. However, it creates a need for additional operations and may leave residual adhesive on the workpiece reducing efficiency and potentially limiting performance.

#### D. SELF SENSING TWEEZERS CONCEPT

In the tweezer application the probes may work in several ways. One of the methods will be discussed and the schematic of operation is presented in Figure 12 where a pair of probes is positioned in static mode (i.e. without excitation) near an object and subsequently picks the object up taking advantage of the attraction forces that are present. The mechanism is then translated to a different location after which the standing wave is turned on and the dynamic force produced being sufficient to overcome the attraction force to enable release.

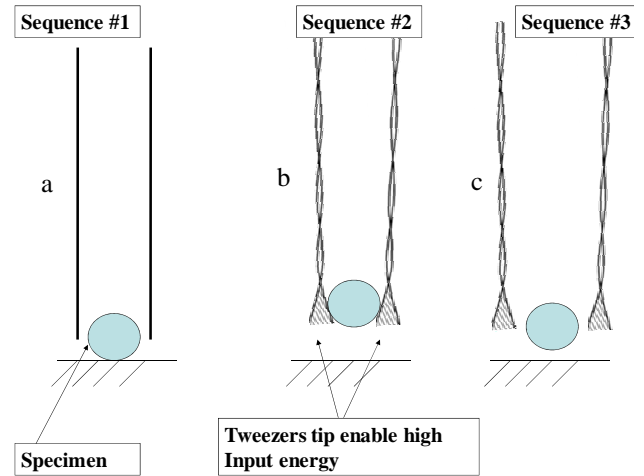


**Figure 12.** Illustration of standing wave tips employed as self sensing tweezers (a) fiber tips are employed in static mode to pick up specimen (b) once the specimen is repositioned the tips are activated using the SW method (b) release occurs once the tip’s combined energy supercedes the attraction bond between the tip(s) and specimen

#### E. TWEEZERS EXPERIMENTAL APPARATUS

A multi-axis platform fashioned from custom built nanopositioning devices, XYZ lift stages, and micrometer positioning stages was constructed. The complete apparatus was equipped with two retractable arms capable of nanometer positioning and each arm was configured with a standing wave sensor as shown by the black and white image of the two sensors on the outside of a 450 $\mu$ m sphere, Figure 12. The objective of this apparatus was intended for pick and release experiments and dimensional metrology experiments. The complete apparatus was assembled inside an enclosed chamber to prevent air flow and minimize dust containments adhering to the tweezers tips, Figure 13. A variety of instrumentation is used ranging from lock-in amplifiers, custom phase lock loop circuits, AC bridge circuitry, oscilloscopes, and data acquisition. Data was collected into a host computer using National Instrument’s LabVIEW. Vision cameras were further employed to provide observation and feedback from the response of the sensor. The cameras enable investigators to see when samples are picked up, released, and interacting with the specimens.

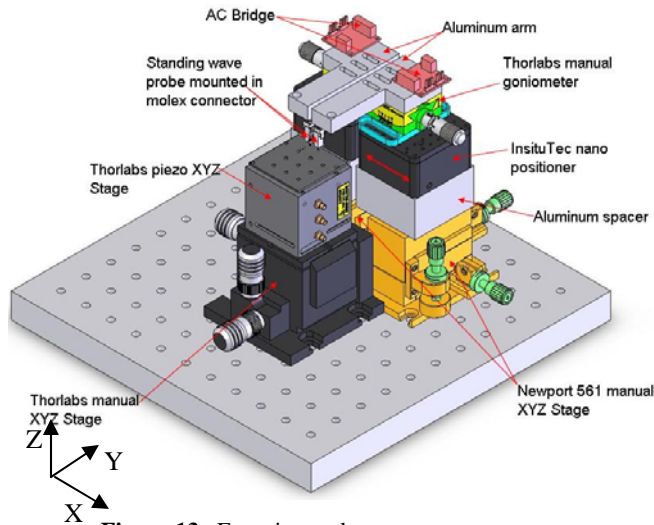


**Figure 13.** Experimental tweezers apparatus.

#### F. SELF SENSING AND MEASUREMENT ABILITY

An extensive amount of work addressed self sensing capability with microscale samples release process was carried out. Specimens were picked up and the standing wave oscillation was turned on with a drive voltage amplitude set at zero volts. In this experiment, the amplitude driving the tuning forks is slowly increased and the output response of one of the tuning forks is measured. Once the standing wave sensor is high enough, the specimen releases and the tuning fork's amplitude Figure 14 and phase Figure 15 signals change. Additionally, the slopes in the amplitude signal are observed to change. From these observations, it is clear the point of release may be determined, the inertia of the sample may be measured based upon the slope of amplitude, and phase may be used to measure release as well.

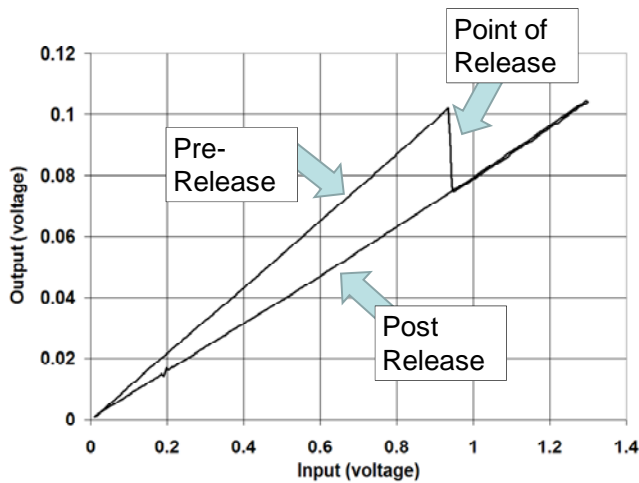


**Figure 14.** Amplitude output vs. Input response for the pick up and release sequence of a glass sphere measured at one arm of the

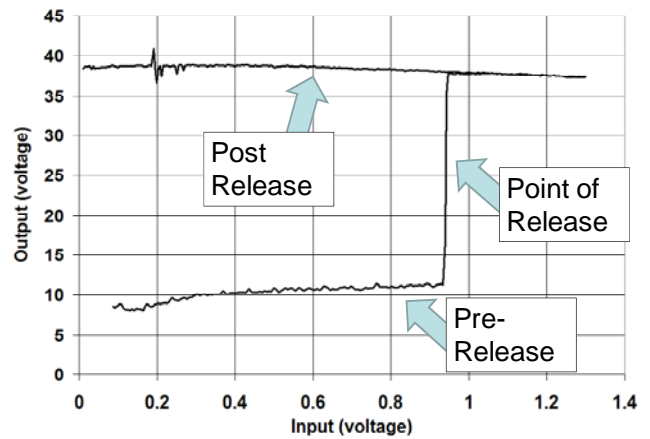


**Figure 15.** Phase output vs. Input response for the pick up and release sequence of a glass sphere measured at one arm of the tweezers.

The experimental station in Fig. 9 is used to assess using dual fibers as dimensional tweezers. To accomplish this goal, the dual tweezers are brought into contact at the tips using independent nanopositioning stages. At this point, both sensors provide a signal and the nanopositioners are both set to zero. This point is referred to as a virtual coordinate established in a 3D space, Figure 16 (right image). Next, the tips positioned away from each other and a  $450\ \mu\text{m}$  sphere is placed in between. The tips are then contacted against the sphere, locked onto a constant force and scanned up the sphere, Figure 16 (left image). The graph in Figure 17, indicates the curvature of the sphere measured by both sensors. This presents interesting issues in dimensional metrology for the MOEMS, as well as MEMS. Essentially, the tool could measure the curvature of optics either before assembly or after. This could serve as a type of in-process inspection tool.

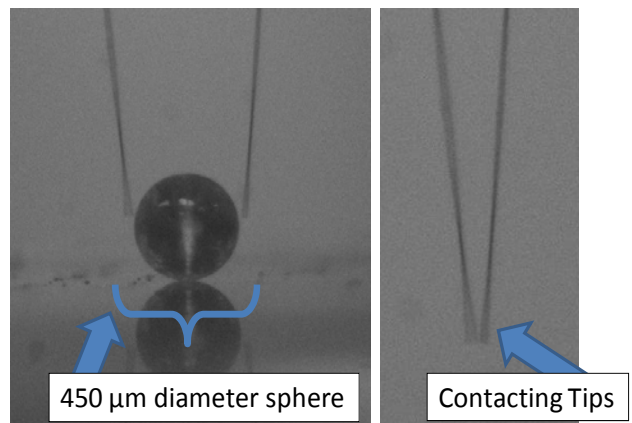


**Figure 16.** Dimensional measurements of microscale sphere using pair of standing wave tweezers (left), establishing of virtual zero by contacting two oscillating tips (right).

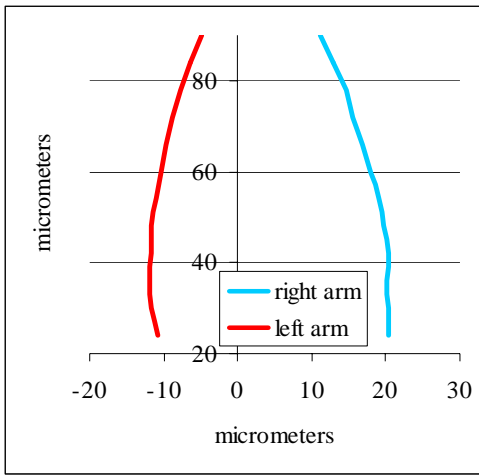


**Figure 17.** Measurement data of microscale sphere, two partial scans of the spherical surface.

#### G. ASSEMBLY WITH MICROSCALE TWEEZERS

Using standing wave tweezers investigations have shown that specimens ranging in size from 10  $\mu\text{m}$  to 500  $\mu\text{m}$  may be picked and released using the standing wave methodology. Above experiments have demonstrated ability to monitor when the specimen is released, measure approximate mass of specimen during release mode and used as a general dimensional sensing tool for metrology inspection (i.e. measure curvature of microscale shapes and inspect quality of assembly process). In addition to the above information authors decided to add a sequence of images showing a assembly of microscale “snowman”, See figures below.

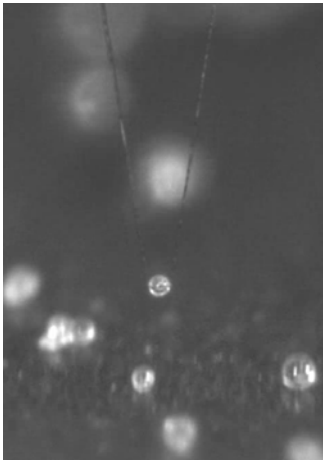


**Figure 18.** Picking up of a 40  $\mu\text{m}$  microscale sphere.

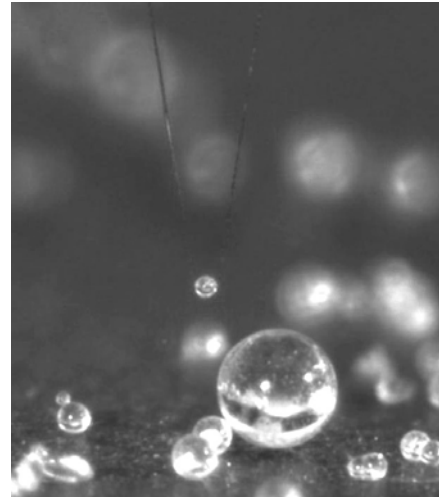


**Figure 19.** Moving of 40  $\mu\text{m}$  microscale sphere.

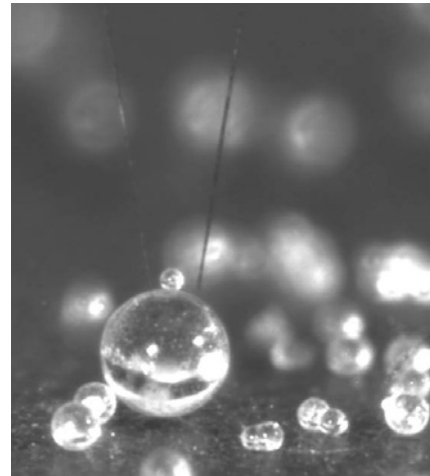


**Figure 20.** Placing 40  $\mu\text{m}$  microscale sphere a top of larger 400  $\mu\text{m}$  sphere, “snowman”

#### CONCLUSIONS

Standing wave technology can be implemented in micro-metrology as well in microassembly. Standing wave probes give a unique opportunity to measure features which are not readily accessible such as microscale holes. Moreover, tweezers build from multiple standing wave probes provide a great way to pick and place microscale objects as well as sense and measure their mass and size. The theoretical studies conducted in parallel with the practical tests show, that building even smaller probes or tweezers based on the same standing wave principal is possible and as a result sensitive nano-tools might be constructed.

#### ACKNOWLEDGMENTS

This work performed under the auspices of the U.S. Department of Energy by Lawrence Livermore National Laboratory under Contract DE-AC52-07NA27344. In addition, the National Institute of Standard and Technology under grant SB134105W0840, and National Science Foundation under grant 0637422.

## REFERENCES

- [1] Jalili N., Laxminarayana K., "A review of atomic force microscopy imaging systems: application to molecular metrology and biological sciences," *Mechatronics* 14, 907-945 (2004).
- [2] Hafner J.H., Cheung C.-L., Woolley A.T., Lieber C.M., "Structural and functional imaging with carbon nanotube AFM probes," *Progress in Biophysics & Molecular Biology* 77, 73-110 (2001).
- [3] Mooney C.B., "Force sensing probes for the Atomic Force Microscope Fabricated by electron beam induced contamination growth" Master Thesis at NCSU, (1997).
- [4] Yang F., "Adhesive contact of axisymmetric suspended miniature structure," *Sensors and Actuators A104*, 44-52 (2003).
- [5] Jones E.E., Begley M.R., Murphy K.D., "Adhesion of micro-cantilevers subjected to mechanical point loading: modeling and experiments," *J. of the Mechanics and Physics of Solids* 51, 1601-1622 (2003).
- [6] Maugis D., "Contact, Adhesion and Rupture of Elastic Solids", *Springer*, (2000).
- [7] Adamson A.W. and Gast, A.P., "Physical Chemistry of Surfaces, 6th Ed.", *Wiley-Interscience*, (1997).
- [8] Israelachvili J.N., "Intermolecular and Surface Forces, 2nd Ed." *Academic Press*, (1992).
- [9] Arnau A., "Piezoelectric Transducers and Applications", *Springer*, (2007).
- [10] Bauza M.B., Hocken R.J., Smith S.T., Woody S.C., "Development of a virtual probe tip with an application to high aspect ratio microscale features," *Rev. Sci. Instrum.* 76, 095112 (2005)
- [11] Bauza M.B., Woody S.C., Smith S.T., Hocken R.J., "Development of a Rapid Profilometer with an Application to Roundness Gauging." *Precision Engineering*. 30 Issue 4; 406-413, (2006)
- [12] Woody S.C., Nowakowski B., Bauza M.B., Smith S.T., "Standing Wave Probes for Microassembly," *Rev. Sci Instrum*, Submitted and accepted for publication (2008)